Conserved functional consequences of disease-associated mutations in the slide helix of Kir6.1 and Kir6.2 subunits of the ATP-sensitive potassium channel

Received for publication, June 30, 2017, and in revised form, August 4, 2017 Published, Papers in Press, August 23, 2017, DOI 10.1074/jbc.M117.804971

Paige E. Cooper[‡1,2], **Conor McClenaghan**[‡1], **Xingyu Chen**[§3], **Anna Stary-Weinzinger**[§4], **and Colin G. Nichols**[‡5]

From the [‡]*Department of Cell Biology and Physiology and Center for the Investigation of Membrane Excitability Diseases, Washington University School of Medicine, St. Louis, Missouri 63110 and* [§]*Department of Pharmacology and Toxicology, University of Vienna, Althanstrasse 14, A-1090 Vienna, Austria*

Edited by F. Anne Stephenson

Cantu syndrome (CS) is a condition characterized by a range of anatomical defects, including cardiomegaly, hyperflexibility of the joints, hypertrichosis, and craniofacial dysmorphology. CS is associated with multiple missense mutations in the genes encoding the regulatory sulfonylurea receptor 2 (SUR2) subunits of the ATP-sensitive K^+ (K_{ATP}) channel as well as two mutations (V65M and C176S) in the Kir6.1 (*KCNJ8*) subunit. Previous analysis of leucine and alanine substitutions at the Val-65-equivalent site (Val-64) in Kir6.2 indicated no major effects on channel function. In this study, we characterized the effects of both valine-to-methionine and valine-to-leucine substitutions at this position in both Kir6.1 and Kir6.2 using ion flux and patch clamp techniques. We report that methionine substitution, but not leucine substitution, results in increased open state stability and hence significantly reduced ATP sensitivity and a marked increase of channel activity in the intact cell irrespective of the identity of the coassembled SUR subunit. Sulfonylurea inhibitors, such as glibenclamide, are potential therapies for CS. However, as a consequence of the increased open state stability, both Kir6.1(V65M) and Kir6.2(V64M) mutations essentially abolish high-affinity sensitivity to the K_{ATP} blocker glibenclamide in both intact cells and excised patches. This raises the possibility that, at least for some CS mutations, sulfonylurea therapy may not prove to be successful and highlights the need for detailed pharmacogenomic analyses of CS mutations.

ATP-sensitive K^+ (K_{ATP})[6] channels, found throughout the body, are generated as octameric complexes consisting of four pore-forming Kir6.1 or Kir6.2 subunits with four regulatory sulfonylurea receptor (SUR1 or SUR2) subunits. SUR1 and Kir6.2 are prominently expressed in the pancreas and neurons, and hence mutations underlie hyperinsulinism, diabetes, and neurological disorders (1). Cantu syndrome (CS) is characterized by a range of apparently disparate features, including cardiomegaly, hyperflexibility of the joints, hypertrichosis, and craniofacial dysmorphology as well as multiple cardiovascular features (2–5). Several reports of missense mutations in the genes encoding the SUR2 and Kir6.1 subunits (*ABCC9* and *KCNJ8*, respectively), which are expressed prominently in cardiovascular tissues, provide strong evidence that CS arises from K_{ATP} gain of function (GOF) (6–10). Gain of function in SUR2- or Kir6.1-containing K_{ATP} channels would be expected to hyperpolarize the membrane potential and decrease excitability, particularly in smooth muscle cells (11). Decreased vascular tone may explain many CS features, including persistent patent ductus arteriosus, dilated and tortuous vessels, lowered blood pressure, increased blood volume, and consequent cardiomegaly.

Although rare, CS is a debilitating syndrome, currently with no specific therapy. Sulfonylureas are potent blockers of K_{ATP} channels. These drugs have proven highly beneficial in treatment of neonatal diabetes resulting from GOF in SUR1- and Kir6.2-dependent channels (12, 13). However, as the molecular defect becomes more severe, the drug effect tends to decline and become ineffective in certain cases (14–17). Whether such effects occur in SUR2- and Kir6.1-dependent channels is not known.

To date, two *KCNJ8* mutations, encoding Kir6.1(V65M) and Kir6.1(C176S), have been reported in association with CS (5, 10). Analogous to residues Cys-166 and Val-64 in Kir6.2, Cys-176 and Val-65 of Kir6.1 are predicted to be positioned in close proximity at the bottom of transmembrane helix 2 (TM2) and the N-terminal slide helix, respectively (see Fig. 1) (18, 19), raising the possibility that mutation of either one increases channel activity by the same mechanism. Interestingly, previous analysis of leucine and alanine substitutions at the equivalent site (Val-64) in Kir6.2 subunit indicated that these substitutions were tolerated without effects on channel function and that such mutations were therefore not causally associated with neonatal diabetes (20). In this study, we sought to resolve the consequences of methionine *versus*

This work was supported in part by National Institutes of Health Grant HL45742 (to C. G. N.). The authors declare that they have no conflicts of interest with the contents of this article. The content is solely the responsibility of the authors and does not necessarily represent the official views of the National Institutes of Health.

[1] Both authors contributed equally to this work.

[2] Supported by National Institutes of Health Training Grant HL007275.
[3] Supported by Austrian Science Fund Grant W1232.
[4] Supported by E-Rare Joint Transnational CantuTreat Program Grant I-2101-B26.

[5] To whom correspondence should be addressed: Dept. of Cell Biology and Physiology Washington University School of Medicine, 660 S. Euclid Ave., St. Louis, MO 63110. Tel.: 314-362-6630; Fax: 314-362-7463; E-mail: cnichols@wustl.edu.

[6] The abbreviations used are: K_{ATP}, ATP-sensitive K^+; CS, Cantu syndrome; SUR, sulfonylurea receptor; GOF, gain of function; TM2, transmembrane helix 2; MI, metabolic inhibition; PIP_2, phosphatidylinositol 4,5-bisphosphate; MD, molecular dynamics; KINT, intracellular potassium.

© 2017 by The American Society for Biochemistry and Molecular Biology, Inc. Published in the U.S.A.

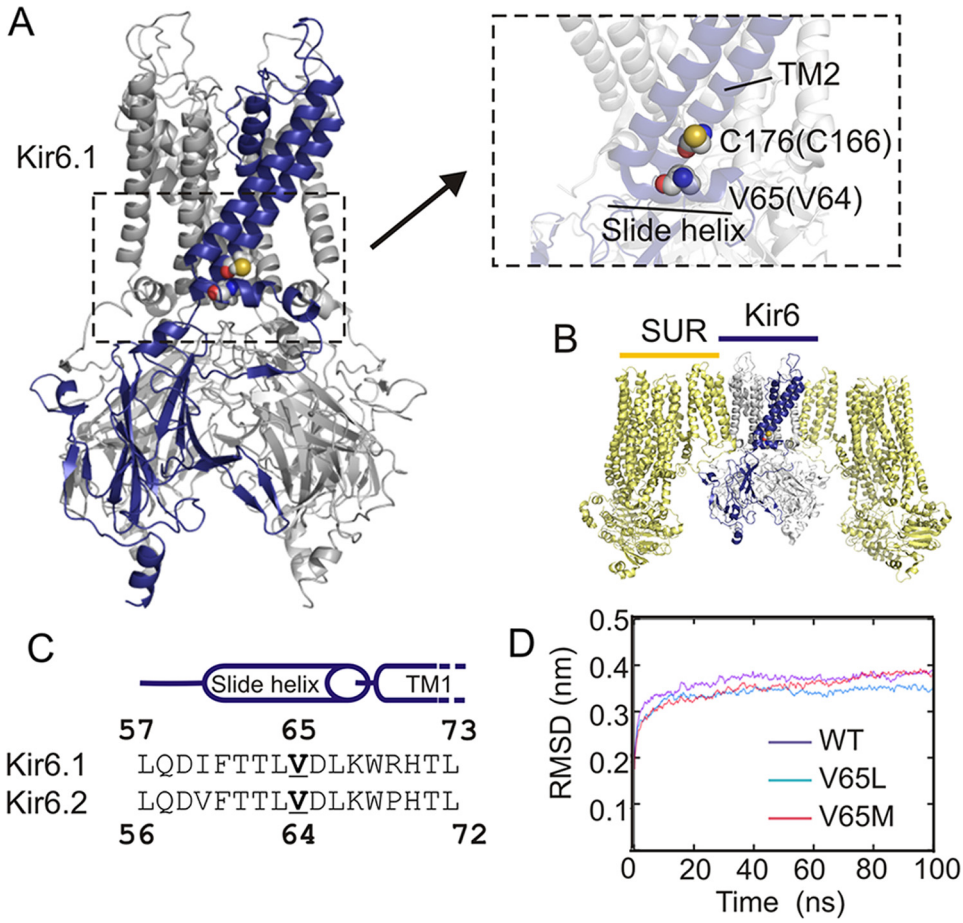

Figure 1. CS-associated mutations in Kir6.1. To date, two mutations in Kir6.1 (*KCNJ8*) have been identified in CS patients, Kir6.1(C176S) and Kir6.1(V65M), at residues that are conserved in Kir6.2. *A*, a Kir6.1 homology model based upon the recent cryo-EM structures for Kir6.2/SUR1 (18, 19) shows that Cys-176 and Val-65 (equivalent to Cys-166 and Val-64 in Kir6.2) lie in close proximity. *Inset*, Val-65 (Val-64) faces TM2 on the slide helix, whereas Cys-176 (Cys-166) lies nearby in TM2. *B*, Kir6.x and SUR subunits coassemble as obligate hetero-octamers in a 1:1 stoichiometry. Here two SUR subunits are omitted for display. *C*, the Kir6.1(V65M) mutation lies in a highly conserved N-terminal sequence within the slide helix. *D*, average root mean square deviation (*RMSD*) from three independent 100-ns MD simulations of the modeled Kir6.1 subunits show that Kir6.1 WT, Kir6.1(V65L), and Kir6.1(V65M) subunits are stable.

leucine substitutions at this position on channel function and sulfonylurea pharmacology.

Results

Kir6.1(V65M), but not Kir6.1(V65L), results in K_{ATP} gain of function

To study recombinant channels containing mutant subunits, COSm6 cells were transfected with WT or mutant Kir6.1 and either SUR1 or SUR2A. Channel activity was first assayed using a radioactive Rb^+ ($^{86}Rb^+$) efflux assay. When expressed with SUR1, Kir6.1(V65M) exhibited markedly increased K_{ATP}-dependent efflux rates compared with WT in both basal conditions (Ringer's solution) and in the presence of the SUR1-selective K_{ATP} activator diazoxide as shown in Fig. 2, *A* and *B*). In contrast, K_{ATP}-dependent efflux rates for Kir6.1(V65L) were not significantly different from WT in either condition (Fig. 2, *A* and *B*).

When K_{ATP} channels were activated by incubation with oligomycin and 2-D-deoxyglucose (metabolic inhibition (MI)), no significant effect on efflux rate was observed for either V65M or V65L (Fig. 2*C*). MI typically leads to maximal activation of all available channels; hence, these results suggest that neither mutation affects the maximal available conductance and therefore that channel density was unaffected. When expressed with SUR2A, the K_{ATP}-dependent basal flux rate was very low for both WT and mutant Kir6.1 subunits (Fig. 3*A*), likely due to lower expression level and decreased Mg-nucleotide activation of the SUR2A subunit (21). However, when channels were activated with the SUR2-selective activator pinacidil, a marked increase in K_{ATP}-dependent flux was seen for V65M-containing, but not V65L-containing, channels, when compared with WT (Fig. 3*B*). Maximum K_{ATP}-dependent efflux rates in MI were significantly higher for V65M than for WT when expressed with SUR2A (Fig. 3*C*). This suggests that V65M increases maximal conductance, although this analysis does not distinguish between increased channel density or more complete activation of available channels.

The conserved effects of valine-to-methionine or -leucine substitution at the equivalent residue in Kir6.2

Val-65 in Kir6.1 and the homologous residue in Kir6.2 (Val-64) lie within the amphipathic N-terminal slide helix, which is highly conserved in Kir channels. As shown in Fig. 4, when coexpressed with SUR1, Kir6.2(V64M) also significantly

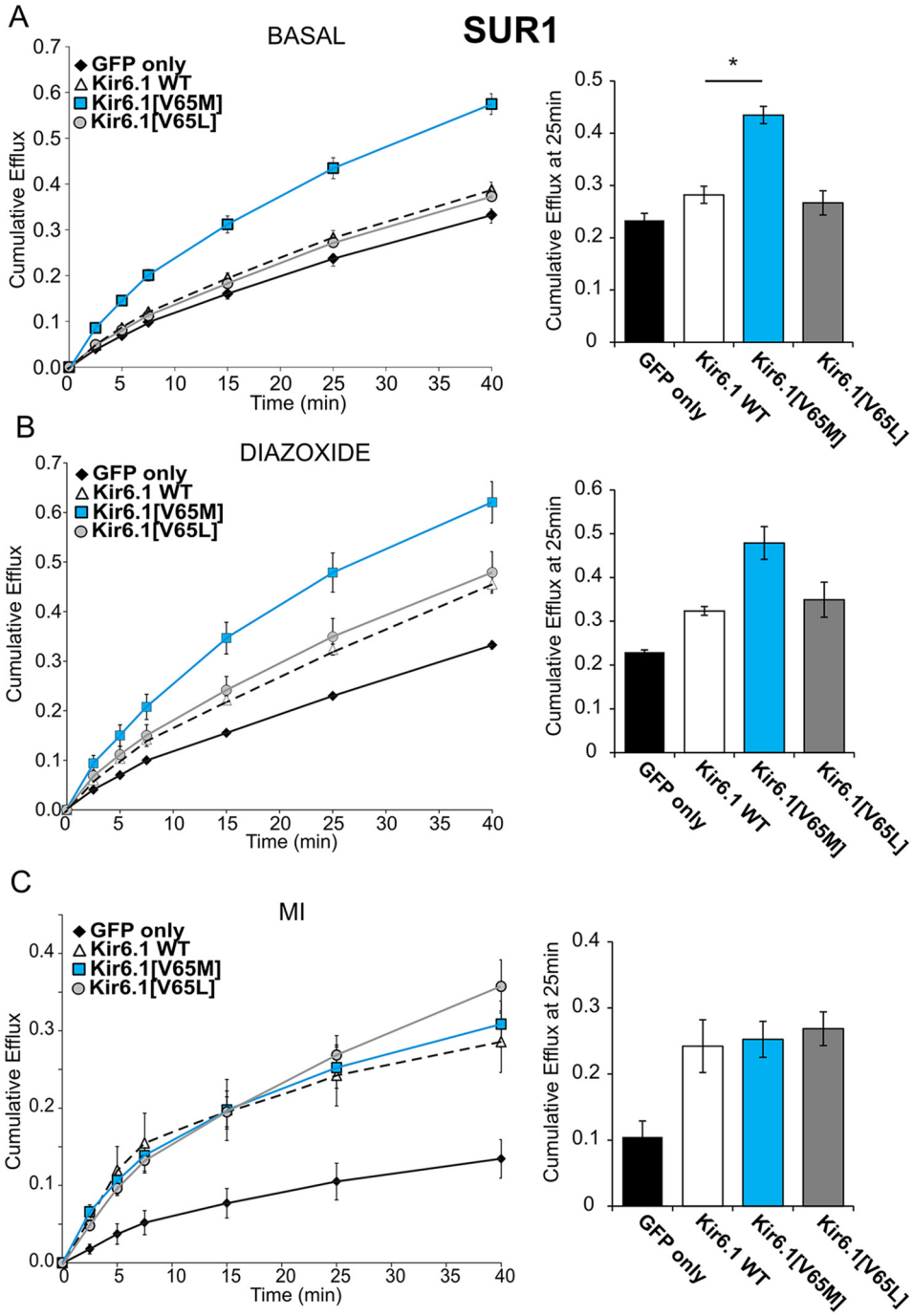

Figure 2. Kir6.1(V65M), but not Kir6.1(V65L), increases SUR1-dependent K_{ATP} channel activity in intact cells. Cumulative $^{86}Rb^+$ efflux as a function of time was measured in GFP-transfected control COSm6 cells and in cells transiently expressing WT or mutant Kir6.1 with SUR1. Experiments were performed in basal conditions in Ringer's solution (*A*) or in the presence of the K^+ channel opener diazoxide (*B*) or the metabolic inhibitors (*MI*) oligomycin and 2-deoxy-D-glucose (*C*). Data points and *error bars* represent mean and S.E. of eight to 18 experiments. Summary representations of the mean cumulative flux at 25 min are shown on the *right* (* denotes statistical significance as determined by unpaired Student's t tests; $p < 0.05$).

increased basal and pinacidil-activated K_{ATP}-dependent efflux rates. Conversely, the V64L mutation had no significant effect, consistent with the previous report that this mutation does not alter channel function (20). When coexpressed with SUR2A, marked increases in basal and pinacidil-activated efflux rates were again observed for Kir6.2(V64M) but not for Kir6.1(V65L) (Fig. 5, *A* and *B*). The same maximum efflux rates in MI for WT, V64M, and V65L, irrespective of the SUR subunit (Figs. 4*C* and 5*C*), imply no effects of either mutation on channel density.

The molecular mechanism of K_{ATP} GOF conferred by valine-to-methionine mutations

Taken together, the above data demonstrate that substitution of valine by methionine at residue 65 in Kir6.1 or residue 64 in Kir6.2 results in gain of function of expressed K_{ATP} channels.

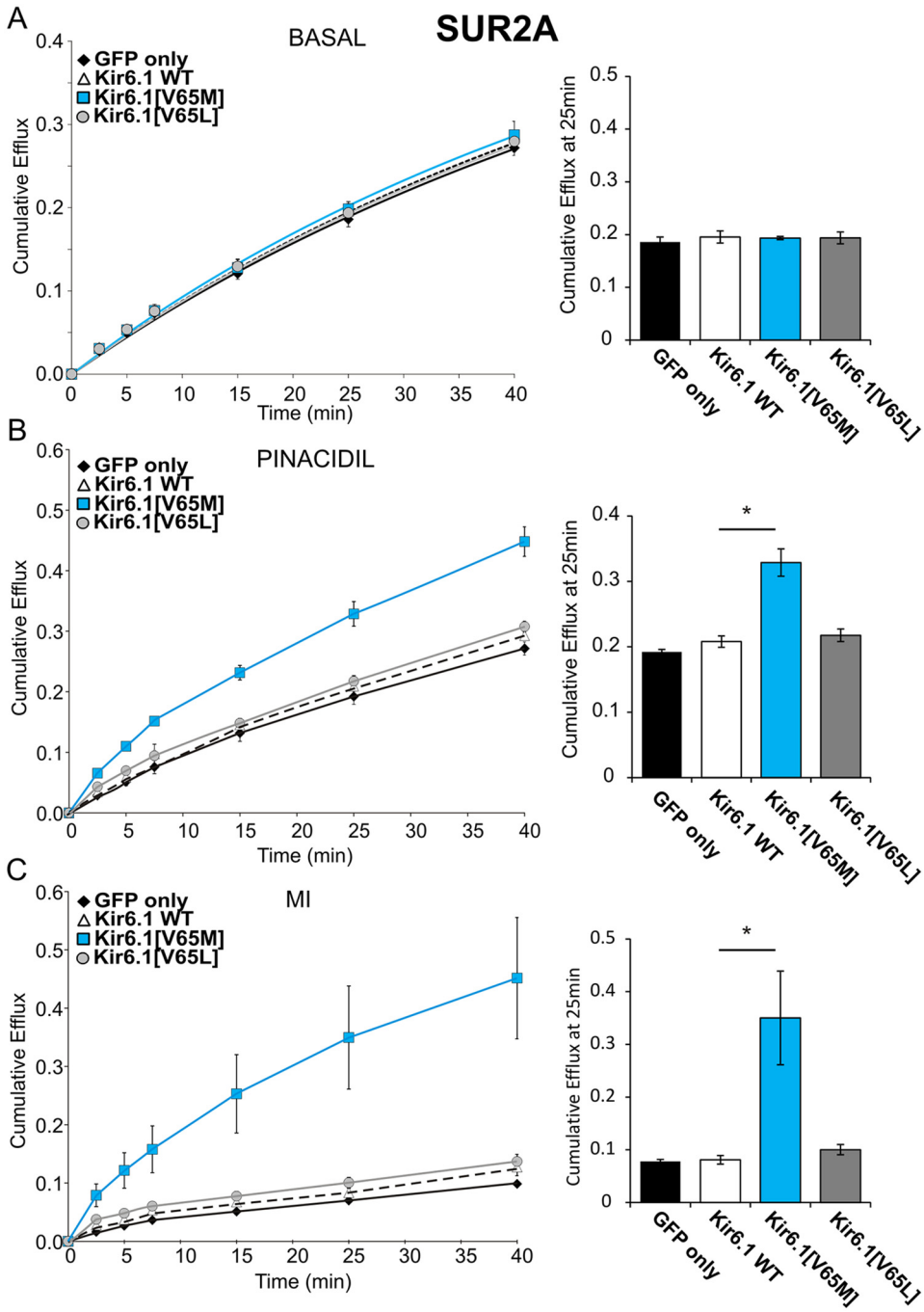

Figure 3. Kir6.1(V65M), but not Kir6.1(V65L), increases SUR2A-dependent K_{ATP} channel activity in intact cells. Cumulative $^{86}Rb^{+}$ efflux as a function of time was measured in GFP-transfected control COSm6 cells and in cells transiently expressing WT or mutant Kir6.1 with SUR2A. Experiments were performed in basal conditions in Ringer's solution (*A*) or in the presence of the K^{+} channel opener pinacidil (*B*) or the metabolic inhibitors (M*I*) oligomycin and 2-deoxy-D-glucose (*C*). Data points and *error bars* represent mean and S.E. of three experiments. Summary representations of the mean cumulative flux at 25 min are shown on the *right* (* denotes statistical significance as determined by Mann-Whitney *U* test; $p < 0.05$).

To investigate the molecular mechanism, we examined nucleotide sensitivity of channels in excised, inside-out patch clamp experiments. As shown in Fig. 6, channels comprising WT Kir6.2 and SUR2A were inhibited by Mg^{2+}-free ATP with an IC_{50} of ~30 μM, which was not significantly altered by the V64L mutation. In contrast, the V64M mutation resulted in ~6-fold reduction in ATP sensitivity (Fig. 6). Decreased ATP sensitivity could arise from a change in the affinity of the channel for ATP or, because ATP binds to and stabilizes closed states of the channel, a change in intrinsic open state stability. Recent cryo-EM structures (18, 19) confirm that the slide helix of Kir6.2 is structurally distinct from the ATP-binding site, and thus a direct effect on ATP binding is not expected. In contrast, multiple studies have demonstrated that mutations in the slide helix act to stabilize open conformations of Kir channels (22–24). PIP_2 in the cytoplasmic leaflet is essential for Kir channel activity (25). At ambient levels in the cytoplasmic leaflet, WT Kir6.2/SUR1 channel open probability is ~0.5 but approaches 1

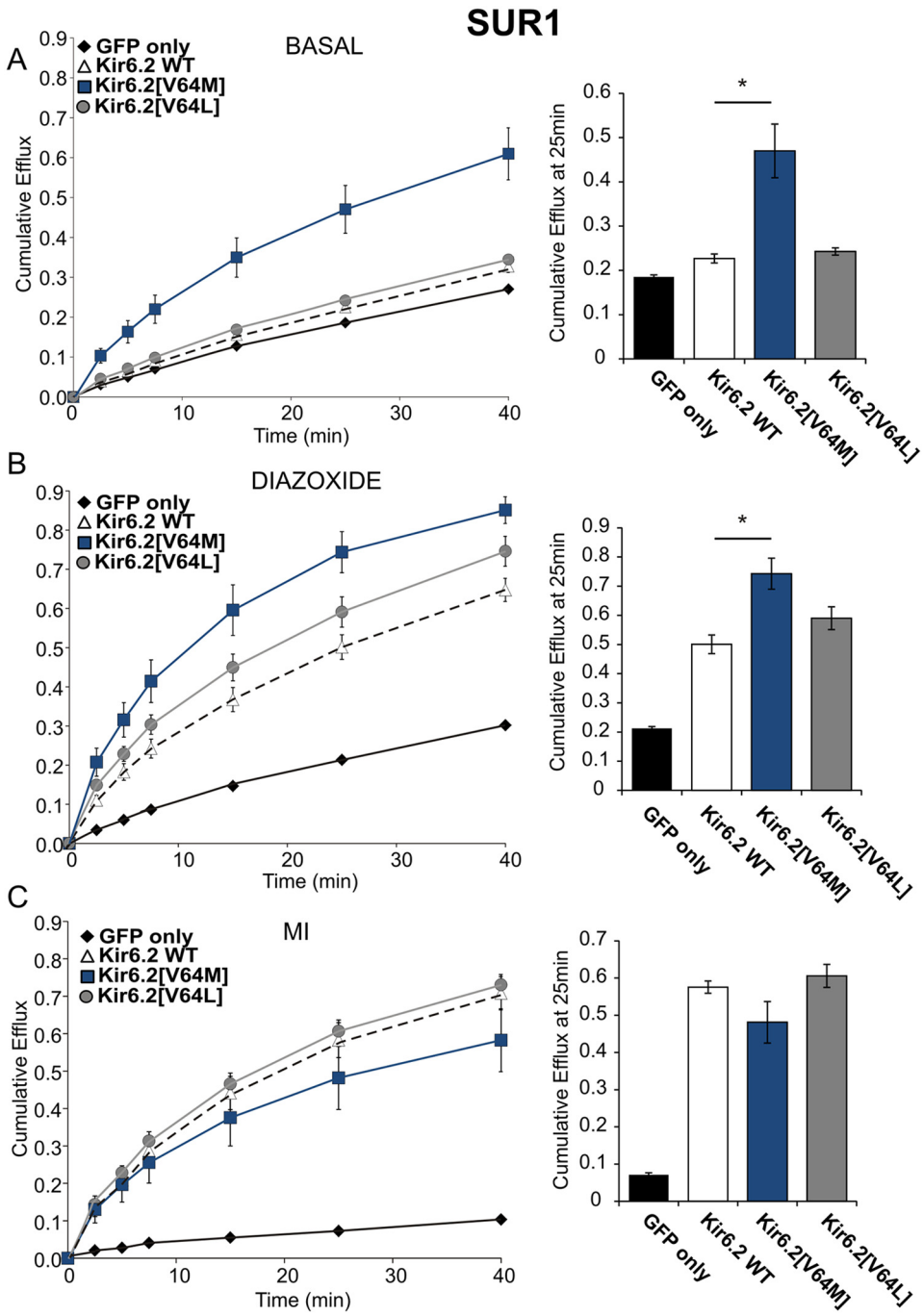

Figure 4. Kir6.2(V64M), but not Kir6.2(V64L), increases SUR1-dependent K_{ATP} channel activity in intact cells. Cumulative $^{86}Rb^+$ efflux as a function of time was measured in GFP-transfected control COSm6 cells and in cells transiently expressing WT or mutant Kir6.2 with SUR1. Experiments were performed in basal conditions in Ringer's solution (*A*) or in the presence of the K^+ channel opener diazoxide (*B*) or the metabolic inhibitors (*MI*) oligomycin and 2-deoxy-D-glucose (*C*). Data points and *error bars* represent mean and S.E. of three to five experiments. Summary representations of the mean cumulative flux at 25 min are shown on the *right* (* denotes statistical significance as determined by Mann-Whitney *U* test; $p < 0.05$).

as PIP_2 is increased in the membrane (26). Mutations that intrinsically stabilize or destabilize the channel open state increase or decrease, respectively, the basal open probability, which can be assessed by maximizing the open probability by adding exogenous PIP_2 (26). To estimate the effect of the V64M mutation on channel open state stability, the activating response to exogenous PIP_2 was therefore assessed for WT Kir6.2- and Kir6.2(V64M)-containing channels (see "Experimental procedures" and Ref. 14). The analysis indicates that the V64M mutation significantly increases the intrinsic apparent P_o under ambient conditions following patch excision (from ~0.6 in WT to ~1.0 in Kir6.2(V64M); Fig. 7, *A–C*).

The open state-stabilizing valine-to-methionine substitutions decrease sulfonylurea sensitivity in both Kir6.2 and Kir6.1

Second generation sulfonylurea drugs, such as glibenclamide, inhibit SUR2-containing K_{ATP} channels with moderate affinity (27, 28) and therefore may serve as a potential pharma-

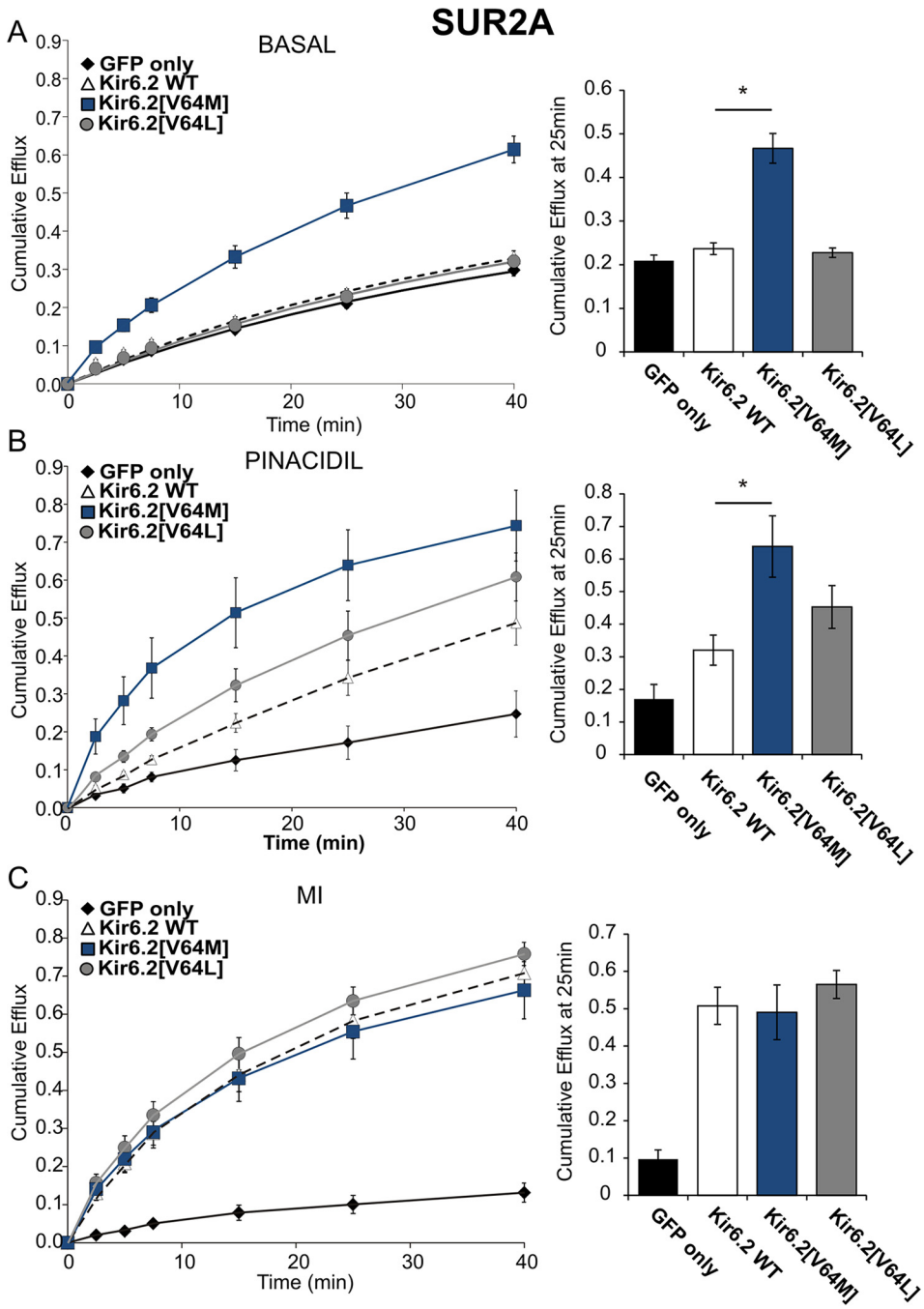

Figure 5. Kir6.2(V64M), but not Kir6.2(V64L), increases SUR2A-dependent K_{ATP} channel activity in intact cells. Cumulative $^{86}Rb^+$ efflux as a function of time was measured in GFP-transfected control COSm6 cells and in cells transiently expressing WT or mutant Kir6.2 with SUR2A. Experiments were performed in basal conditions in Ringer's solution (*A*) or in the presence of the K^+ channel opener pinacidil (*B*) or the metabolic inhibitors (*MI*) oligomycin and 2-deoxy-D-glucose (*C*). Data points and *error bars* represent mean and S.E. of three to six experiments. Summary representations of the mean cumulative flux at 25 min are shown on the *right* (* denotes statistical significance as determined by Mann-Whitney *U* test; $p < 0.05$).

cotherapy for CS. However, it has previously been demonstrated that open state-stabilizing mutations in Kir6.x subunits can impair sulfonylurea inhibition (14–16). The effect of 10 μM glibenclamide on K_{ATP}-dependent rubidium effluxes was assessed in cells expressing either WT or V64M mutant Kir6.2 with SUR2A. As shown in Fig. 8, MI-activated WT channel fluxes were inhibited ~75% by glibenclamide, but there was no significant inhibition of Kir6.2(V64M) channels.

All known CS patients are heterozygous, and we modeled heterozygosity by cotransfecting WT and V64M mutant Kir6.2 with SUR2A subunits. Glibenclamide inhibition was again markedly reduced by the V64M mutation with only ~20% inhibition of MI-activated Rb^+ fluxes (Fig. 8, *A* and *B*). We also examined the sensitivity of Kir6.2 + SUR2A and Kir6.2(V64M) + SUR2A channels to glibenclamide inhibition in inside-out patch clamp recordings (Fig. 8, *C* and *D*). In agreement with the above results, sensitivity was again markedly reduced by the V64M mutation (Fig. 8, *C* and *D*) with almost no inhibition even at 10 μM glibenclamide.

As the open state-stabilizing effects appear to be similar for the Kir6.2(V64M) and Kir6.1(V65M) mutations, the effects of

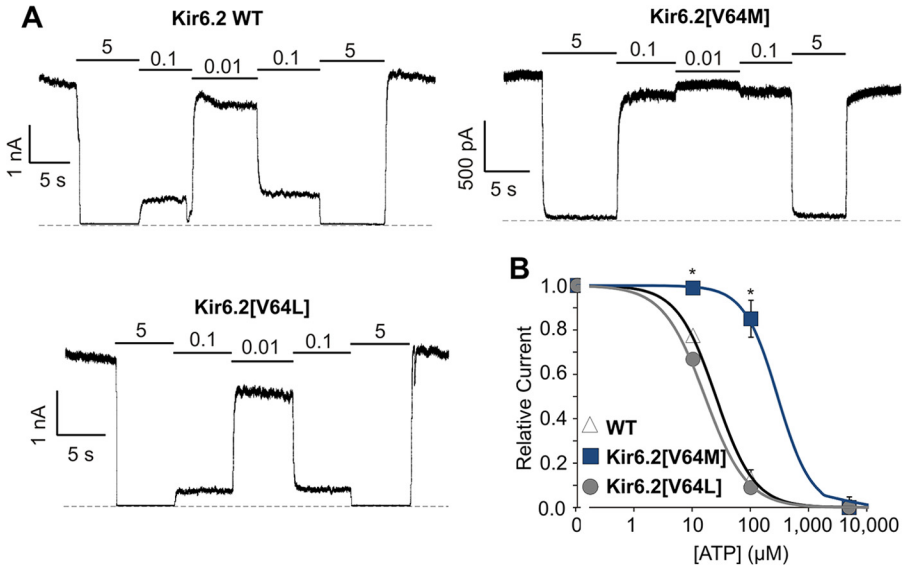

Figure 6. Gain of function in Kir6.2(V64M) results from decreased ATP sensitivity. Representative excised patch clamp recordings from COSm6 cells coexpressing WT or mutant Kir6.2 subunits with SUR2A are shown. *A*, membrane potential was held at −50 mV, and currents were recorded continuously in inside-out excised patches exposed to KINT in the absence or presence of 0.01, 0.1, or 5 mM Mg^{2+}-free ATP. *B*, summary dose-response data (data points and *error bars* represent mean and S.E.; 10 patches each) was fit using a four-parameter Hill equation to estimate the ATP concentration for half-maximal inhibition. IC_{50} values were 32.2 ± 6.6 μM (Hill coefficient, 2.2 ± 0.2) for WT, 198 ± 31.1 μM (Hill coefficient, 2.9 ± 0.3) for Kir6.2(V64M), and 31.0 ± 2.2 μM (Hill coefficient, 2.2 ± 0.1) for Kir6.2(V64L) (* denotes statistical significance as determined by unpaired Student's t tests; $p < 0.05$). In this and in representative current recordings in subsequent figures, the *dashed lines* represent zero channel current.

mutations on inhibitor sensitivity are also likely to be conserved. However, a previous report suggested that sulfonylurea sensitivity may be differentially affected by mutations in the slide helix of Kir6.2 *versus* Kir6.1 (15). Thus, we also sought to confirm the effect of the Kir6.1(V65M) mutation itself on glibenclamide inhibition. Due to very low Rb^+ fluxes and low density in patch-clamp recordings for Kir6.1-only-containing channels, we coexpressed Kir6.1 WT or Kir6.1(V65M) with WT Kir6.2 to yield heterotetramers as described previously (10). As expected, heteromeric Kir6.2/Kir6.1(V65M) channels exhibited ~5-fold lower ATP sensitivity in excised patch clamp recordings than Kir6.2/Kir6.1 WT channels (Fig. 9*A*). In Rb^+ flux experiments, the effect of 10 μM glibenclamide on K_{ATP}-dependent efflux was also reduced from ~50% for WT Kir6.1-containing channels to ~30% for V65M-containing channels (Fig. 9, *C* and *D*), and glibenclamide sensitivity was markedly reduced in Kir6.2/Kir6.1(V65M) channels in inside-out patch clamp recordings (Fig. 9, *E* and *F*).

Discussion

The recent identification of multiple missense mutations in SUR2 (*ABCC9*) and Kir6.1 (*KCNJ8*), which all result in K_{ATP} GOF, demonstrates that CS arises primarily from K_{ATP} channel GOF (2, 10). Brownstein *et al.* (5) initially reported the Kir6.1(V65M) mutation in a case report with the prediction that the mutation was causal. However, a previous report showed that other substitutions at the equivalent (Val-64) residue in Kir6.2 are tolerated without significant effects on K_{ATP} function (20). This raises the possibility that the Kir6.1(V65M) mutation may actually be benign. To address this, we systematically characterized the effects of valine-to-methionine and valine-to-leucine substitutions in both Kir6.1 and Kir6.2 and show that methionine substitution, but not leucine substitution, results in marked gain of function for either channel, whether coexpressed with SUR1 or SUR2A regulatory subunits. We show that substitution by methionine, but not by leucine, results in reduced ATP sensitivity for both Kir6.2(V64M) and Kir6.1(V65M) channels, and for Kir6.2(V64M), we show that this results from an increase in the open state stability such that the intrinsic open probability is higher. As a consequence, K_{ATP} channels that include this mutation will exhibit increased activity under physiological regulation by intracellular nucleotides. Similar increases in open state stability have previously been reported for other slide helix mutations (*e.g.* Q52R (14)), reflecting an important role of this domain in controlling channel gating. Intriguingly, in light of recently reported structures of the Kir6.2-SUR1 K_{ATP} complex (18, 19), the single other known CS Kir6.1 mutation, Kir6.1(C176S), is located very close to Val-65 in a cluster of hydrophobic residues (Fig. 1). Previous analyses have demonstrated that the equivalent Kir6.2(C166S) also increases intrinsic open state stability (29, 30). This raises the possibility that both V65M and C176S mutations act to destabilize the closed channel by disrupting this closed-state hydrophobic cluster. In contrast, Männikkö *et al.* (20) reported that the Kir6.2(V64L) mutation ameliorated the deleterious effects of the nearby pathogenic F60Y mutation when expressed on the same subunit. Thus, it is also possible that V64M may result in pathogenic reduction of ATP sensitivity by disrupting the interaction that is normally present between these two slide helix residues.

The potential utility of sulfonylurea drugs in the treatment of CS remains to be tested clinically, but "second-generation" sulfonylureas, such as glibenclamide (glyburide), which demonstrate moderate potency for inhibiting SUR2-containing K_{ATP} channels, may offer promise for a specific therapy. However,

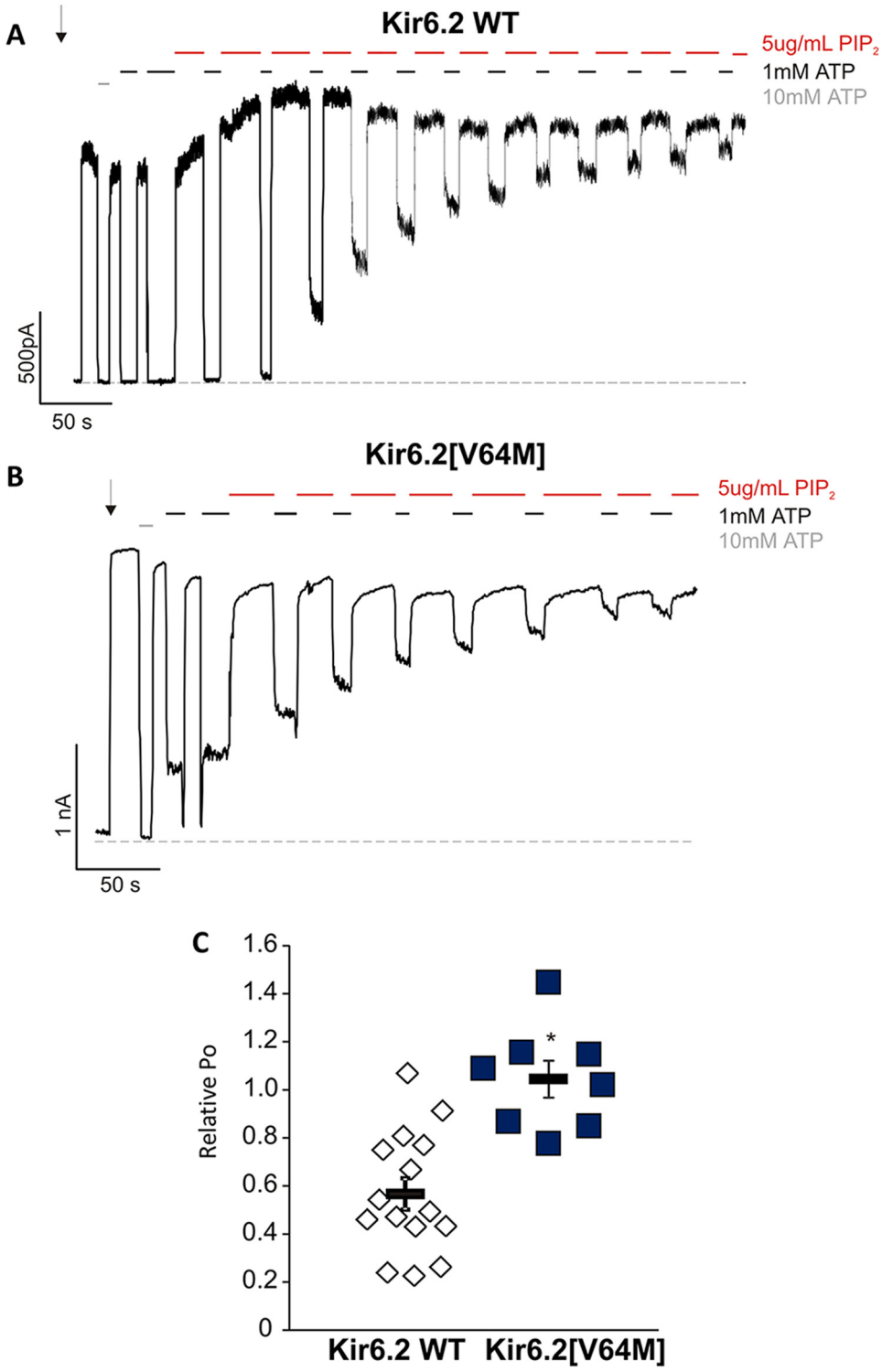

Figure 7. Kir6.2(V64M) increases channel open state stability. Representative K_{ATP} currents recorded from patches expressing WT (*A*) or V64M mutant Kir6.2 (*B*) with SUR2A following excision at the *arrow* and in the presence of 10 mM ATP, 1 mM ATP, or 5 μg/ml PIP_2 as indicated are shown. *C*, relative P_o determined as a ratio of steady-state current in the patch upon excision in the absence of nucleotides to the maximum current measured following PIP_2. Individual patch data are represented by *symbols* ($n = 8–14$); *bars* and *error bars* are the means and S.E. Relative $P_o = 0.59 \pm 0.07$ (WT) and 1.05 ± 0.07 (Kir6.2(V64M)) (* denotes statistical significance as determined by unpaired Student's *t* tests; $p < 0.05$).

sulfonylurea sensitivity can be markedly decreased by K_{ATP} mutations that increase the intrinsic open probability of channels (14–16). Consistent with this, we show here that both the Kir6.1(V65M) and Kir6.2(V64M) mutations essentially abolish high-affinity glibenclamide sensitivity in both intact cells and excised patches. This finding raises the possibility that, at least for some CS mutations, sulfonylurea therapy may not be successful and highlights the need for detailed pharmacogenomic analyses of the effects of individual CS mutations on K_{ATP} inhibitor sensitivity.

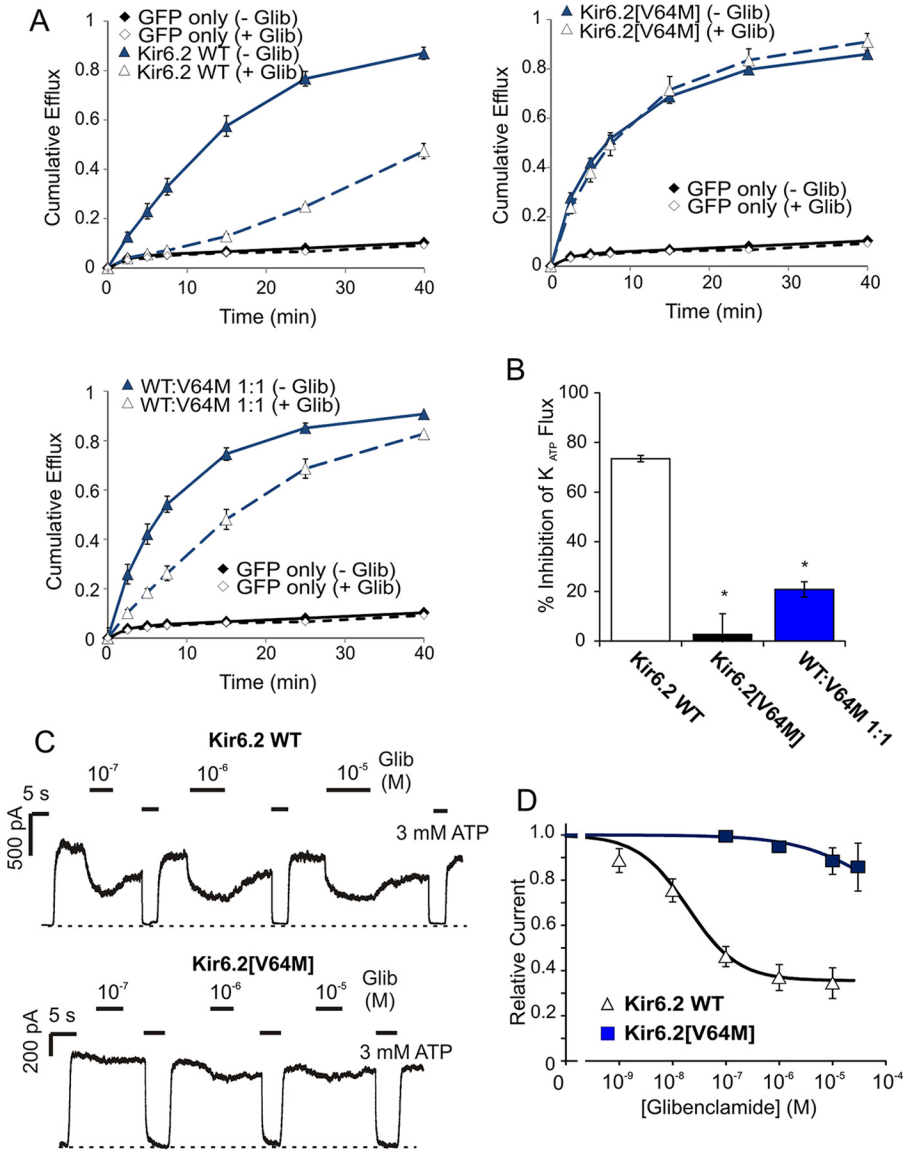

Figure 8. Kir6.2(V64M) decreases glibenclamide sensitivity in intact cells and excised patches. Cumulative $^{86}Rb^+$ efflux as a function of time was measured from COSm6 cells incubated in metabolic inhibitors oligomycin and 2-deoxy-D-glucose in the presence or absence of 10 μM glibenclamide (*Glib*). *A*, *top left*, cells were transfected either with GFP alone or with WT Kir6.2 and SUR2A. *Top right*, cells were transfected either with GFP alone or with Kir6.2(V64M) and SUR2A. *Bottom left*, cells were transfected either with GFP alone or with a 1:1 mixture of Kir6.2 WT and Kir6.2(V64M) plus SUR2A. Data points and *error bars* represent mean and S.E. of three experiments. *B*, percent inhibition of K_{ATP} flux at the 25-min time point from three independent experiments. *C*, representative traces from inside-out patch clamp recordings from cells transfected with Kir6.2 WT and SUR2A (*top* trace) or Kir6.2(V64M) and SUR2A (*bottom* trace) at −50 mV in the presence and absence of 3 mM ATP or increasing concentrations of glibenclamide as indicated. *D*, summary glibenclamide dose response from inside-out patch recordings (data points and *error bars* represent mean and S.E. from three to five patches). *Asterisks* (*) denote statistical significance as determined by Mann-Whitney *U* test ($p < 0.05$).

Experimental procedures

Modeling of Kir6.1 tetrameric channels

Kir6.1 was modeled by homology to the recently published Kir6.2 structures Protein Data Bank code 5TWV (19) and Protein Data Bank code 5WUA (18). Molecular dynamics (MD) simulations were carried out using Gromacs software version 5.1.1 and the Amber 99 force field as described previously (31). Mutations were introduced using Swiss-PdbViewer (32). Three 100-ns MD simulations were performed for WT Kir6.1 and V65L and V65M mutants. All structures were embedded in a lipid bilayer consisting of 588 1-palmitoyl-2-oleoylphosphatidylcholine lipids using the g_membed tool (33) and solvated using the extended simple point charge water model (34). K^+ and Cl^- ions were randomly placed within the solvent to neutralize the system and to obtain an ion concentration of 150 mM. The root mean square deviation of simulated protein structures all converged to ~3.5 Å for each structure at around 20 ns, indicating that the simulated systems were stable and at equilibrium (Fig. 1*D*).

Mutagenesis and heterologous expression of K_{ATP} channels

Mutations were introduced in rat Kir6.1-pcDNA3.1 and mouse Kir6.2-pcDNA3.1 using the QuikChange II site-directed mutagenesis kit (Agilent Technologies) and confirmed by direct sequencing of the coding region. For channel expression, COSm6 cells were cultured in Dulbecco's modified Eagle's medium (DMEM) supplemented with 10% fetal bovine serum,

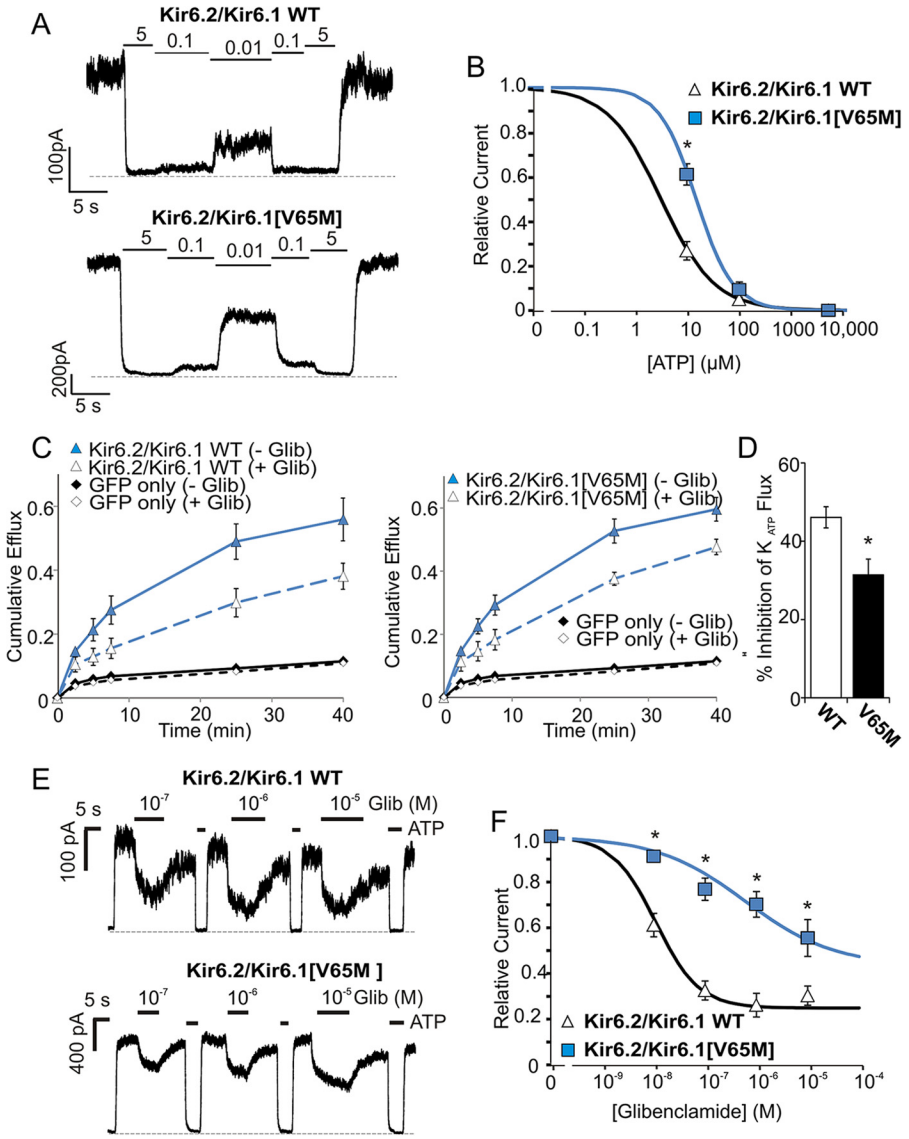

Figure 9. The Kir6.1(V65M) mutation decreases glibenclamide sensitivity in heterotetrameric channels expressed in intact cells and excised patches. *A*, representative inside-out patch current recordings from COSm6 cells transfected with a 1:1 mixture of Kir6.2 WT and either Kir6.1 WT (*top*) or Kir6.1(V65M) (*bottom*) and SUR2A. *B*, summary dose-response data (mean ± S.E. from three patches) was fit using a four-parameter Hill equation to estimate the ATP concentration for half-maximal inhibition.The IC_{50} for Kir6.2 WT/Kir6.1 WT-containing channels was 3.2 ± 1.2 μM (Hill coefficient 0.9 ± 0.1; $n = 3$) compared with 15.1 ± 2.6 μM (Hill coefficient 1.2 ± 0.1; $n = 3$) for Kir6.2 WT/Kir6.1(V65M)-containing channels (* denotes statistical significance as determined by Mann-Whitney *U* tests; $p < 0.05$). *C*, cumulative $^{86}Rb^+$ efflux as a function of time was measured from COSm6 cells incubated in metabolic inhibitors oligomycin and 2-deoxy-D-glucose in the presence or absence of 10 μM glibenclamide (*Glib*). *Left*, cells were transfected either with GFP alone or with a 1:1 ratio of Kir6.2 WT with Kir6.1 WT and SUR2A. *Right*, cells were transfected either with GFP alone or with a 1:1 ratio of Kir6.2 WT with Kir6.1(V65M) and SUR2A. Data points and *error bars* represent mean and S.E. of three experiments. *D*, the inhibition of K_{ATP} flux by 10 μM glibenclamide (calculated as in Fig. 8). Kir6.2 WT/Kir6.1 WT-containing channels were inhibited by 46.1 ± 2.7% compared with 31.4 ± 4.0% for Kir6.2 WT/Kir6.1(V65M)-containing channels. *E*, representative traces from inside-out patch clamp recordings from cells transfected with Kir6.2 WT/Kir6.1 WT and SUR2A (*top* trace) or Kir6.2 WT/Kir6.1(V65M) and SUR2A (*bottom* trace). Currents were recorded at −50 mV in the presence and absence of 3 mM ATP or increasing concentrations of glibenclamide as indicated. *F*, summary glibenclamide dose response from inside-out patch clamp recordings (data points and *error bars* represent mean and S.E. from three patches). *Asterisks* (*) denote statistical significance as determined by Mann-Whitney *U* test ($p < 0.05$).

10^5 units/liter penicillin, and 100 mg/liter streptomycin. At 60–70% confluence, cells were transfected with the relevant plasmids using FuGENE 6 transfection reagent (Promega). For experiments with homomeric channels, cells were cotransfected with pcDNA3.1-mKir6.2 or pcDNA3-Kir6.1 (0.6 μg) and pECE-hamsterSUR1 cDNA or pCMV6-ratSUR2A (SUR2) (1 μg). For experiments using heteromeric channels, cells were cotransfected with WT and mutant Kir6.x with WT SURx at ratios of 0.3:0.3:1.0 (w/w/w). Cells transfected with GFP-pcDNA3.1 served as controls. A small amount of GFP DNA was coexpressed for identification of transfected cells in electrophysiology experiments.

Macroscopic $^{86}Rb^+$ efflux assays

Transfected cells were incubated overnight at 37 °C in DMEM containing 1 μCi/ml ^{86}RbCl (PerkinElmer Life Sciences). Bathing medium was then replaced by room temperature Ringers solution (118 mM NaCl, 10 mM HEPES, 25 mM $NaHCO_3$, 4.7 mM KCl, 1.2 mM KH_2PO_4, 2.5 mM $CaCl_2$, 1.2 mM $MgSO_4$, adjusted to pH 7.4 with NaOH) immediately before

two 1-min washes in assay medium. ^{86}Rb efflux was then assessed in 1) the absence (basal) or 2) presence of 2.5 mg/ml oligomycin and 1 mmol/liter 2-deoxy-D-glucose (metabolic inhibition; applied during two 1-min washes prior to assay) or 3) the presence of SUR1- or SUR2-specific K^+ channel opener, diazoxide or pinacidil, respectively, at 100 μM (applied during two 1-min washes prior to assay). At selected time points, the solution was collected and replaced with fresh solution. Upon completion of the assay, cells were lysed with 2% SDS, and radioactivity in these samples was measured by liquid scintillation. A nonspecific efflux pathway was assumed to be present in all experiments. In metabolic inhibition in particular, both the nonspecific efflux rate and K_{ATP}-specific efflux rates decreased with time. Data are shown as mean cumulative Rb^+ efflux (±S.E.) relative to total initial Rb^+ content. Data were tested for statistical significance using the Student's *t* test where normal distribution of data could be confirmed or by the non-parametric Mann-Whitney *U* test where normal distribution could not be confirmed; a *p* value <0.05 was considered significant for both tests.

Excised patch clamp

After 24–48 h, transfected fluorescent cells were selected for analysis by excised patch clamp experiments using a perfusion chamber that allows for the rapid switching of solutions (35). The bath and pipette solutions (KINT) contained 140 mM KCl, 10 mM HEPES, 1 mM EGTA, pH 7.4 with KOH. K_{ATP} currents were recorded from inside-out patches at −50 mV. Current levels in solutions of varying nucleotide or glibenclamide concentrations were normalized to the basal current in the absence of inhibitors, and dose-response data were fit with a four-parameter Hill equation.

$$\text{Normalized current} = I_{min} + (I_{max} - I_{min})/(1 + ([X]/IC_{50})^H) \quad \text{(Eq. 1)}$$

where the current in KINT = I_{max}, I_{min} is the minimum current observed in high ATP, [*X*] refers to the concentration of ATP or glibenclamide, IC_{50} is the concentration of half-maximal inhibition, and *H* denotes the Hill coefficient.

For experiments assessing PIP_2 activation, an ammonium salt of L-α-phosphatidylinositol 4,5-bisphosphate from porcine brain (Avanti Polar Lipids) was dissolved in KINT to prepare a 5 μg/ml working solution. For each membrane patch, P_o was estimated by dividing the steady-state current in zero ATP by the maximum steady-state current after exposure to PIP_2 (14). Data were tested for statistical significance using Student's *t* test where normal distribution of data could be confirmed or by the non-parametric Mann-Whitney *U* test where normal distribution could not be confirmed. A *p* value <0.05 was considered significant for both tests. Experiments were performed at 20–22 °C.

Author contributions—P. C. and C. G. N. conceived the project. P. C., C. M., and C. G. N. designed the experiments. P. C., C. M., and X. C. performed the experiments and analyzed the data. P. C., C. M., A. S.-W., and C. G. N. wrote the paper.

Acknowledgment—The computational simulations were carried out using the Vienna Scientific Cluster.

References

1. Nichols, C. G. (2006) K_{ATP} channels as molecular sensors of cellular metabolism. *Nature* **440,** 471–476
2. Nichols, C. G., Singh, G. K., and Grange, D. K. (2013) K_{ATP} channels and cardiovascular disease: suddenly a syndrome. *Circ. Res.* **112,** 1059–1072
3. Levin, M. D., Singh, G. K., Zhang, H. X., Uchida, K., Kozel, B. A., Stein, P. K., Kovacs, A., Westenbroek, R. E., Catterall, W. A., Grange, D. K., and Nichols, C. G. (2016) K_{ATP} channel gain-of-function leads to increased myocardial L-type Ca^{2+} current and contractility in Cantu syndrome. *Proc. Natl. Acad. Sci. U.S.A.* **113,** 6773–6778
4. Leon Guerrero, C. R., Pathak, S., Grange, D. K., Singh, G. K., Nichols, C. G., Lee, J. M., and Vo, K. D. (2016) Neurologic and neuroimaging manifestations of Cantu syndrome: a case series. *Neurology* **87,** 270–276
5. Brownstein, C. A., Towne, M. C., Luquette, L. J., Harris, D. J., Marinakis, N. S., Meinecke, P., Kutsche, K., Campeau, P. M., Yu, T. W., Margulies, D. M., Agrawal, P. B., and Beggs, A. H. (2013) Mutation of KCNJ8 in a patient with Cantu syndrome with unique vascular abnormalities—support for the role of K(ATP) channels in this condition. *Eur. J. Med. Genet.* **56,** 678–682
6. Harakalova, M., van Harssel, J. J., Terhal, P. A., van Lieshout, S., Duran, K., Renkens, I., Amor, D. J., Wilson, L. C., Kirk, E. P., Turner, C. L., Shears, D., Garcia-Minaur, S., Lees, M. M., Ross, A., Venselaar, H., *et al.* (2012) Dominant missense mutations in ABCC9 cause Cantú syndrome. *Nat. Genet.* **44,** 793–796
7. van Bon, B. W., Gilissen, C., Grange, D. K., Hennekam, R. C., Kayserili, H., Engels, H., Reutter, H., Ostergaard, J. R., Morava, E., Tsiakas, K., Isidor, B., Le Merrer, M., Eser, M., Wieskamp, N., de Vries, P., *et al.* (2012) Cantu syndrome is caused by mutations in ABCC9. *Am. J. Hum. Genet.***90,** 1094–1101
8. Afifi, H. H., Abdel-Hamid, M. S., Eid, M. M., Mostafa, I. S., and Abdel-Salam, G. M. (2016) *De novo* mutation in ABCC9 causes hypertrichosis acromegaloid facial features disorder. *Pediatr. Dermatol.* **33,** e109–e113
9. Cooper, P. E., Sala-Rabanal, M., Lee, S. J., and Nichols, C. G. (2015) Differential mechanisms of Cantu syndrome-associated gain of function mutations in the ABCC9 (SUR2) subunit of the K_{ATP} channel. *J. Gen. Physiol.* **146,** 527–540
10. Cooper, P. E., Reutter, H., Woelfle, J., Engels, H., Grange, D. K., van Haaften, G., van Bon, B. W., Hoischen, A., and Nichols, C. G. (2014) Cantu syndrome resulting from activating mutation in the KCNJ8 gene. *Hum. Mutat.* **35,** 809–813
11. Li, A., Knutsen, R. H., Zhang, H., Osei-Owusu, P., Moreno-Dominguez, A., Harter, T. M., Uchida, K., Remedi, M. S., Dietrich, H. H., Bernal-Mizrachi, C., Blumer, K. J., Mecham, R. P., Koster, J. C., and Nichols, C. G. (2013) Hypotension due to Kir6.1 gain-of-function in vascular smooth muscle. *J. Am. Heart Assoc.* **2,** e000365
12. Wambach, J. A., Marshall, B. A., Koster, J. C., White, N. H., and Nichols, C. G. (2010) Successful sulfonylurea treatment of an insulin-naive neonate with diabetes mellitus due to a KCNJ11 mutation. *Pediatr. Diabetes* **11,** 286–288
13. Pearson, E. R., Flechtner, I., Njølstad, P. R., Malecki, M. T., Flanagan, S. E., Larkin, B., Ashcroft, F. M., Klimes, I., Codner, E., Iotova, V., Slingerland, A. S., Shield, J., Robert, J. J., Holst, J. J., Clark, P. M., *et al.* (2006) Switching from insulin to oral sulfonylureas in patients with diabetes due to Kir6.2 mutations. *N. Engl. J. Med.* **355,** 467–477
14. Koster, J. C., Remedi, M. S., Dao, C., and Nichols, C. G. (2005) ATP and sulfonylurea sensitivity of mutant ATP-sensitive K^+ channels in neonatal diabetes: implications for pharmacogenomic therapy. *Diabetes* **54,** 2645–2654
15. Winkler, M., Lutz, R., Russ, U., Quast, U., and Bryan, J. (2009) Analysis of two KCNJ11 neonatal diabetes mutations, V59G and V59A, and the analogous KCNJ8 I60G substitution: differences between the channel subtypes formed with SUR1. *J. Biol. Chem.* **284,** 6752–6762
16. Proks, P., de Wet, H., and Ashcroft, F. M. (2013) Molecular mechanism of sulphonylurea block of K_{ATP} channels carrying mutations that impair ATP inhibition and cause neonatal diabetes. *Diabetes* **62,** 3909–3919

17. McTaggart, J. S., Clark, R. H., and Ashcroft, F. M. (2010) The role of the K_{ATP} channel in glucose homeostasis in health and disease: more than meets the islet. *J. Physiol.* **588,** 3201–3209
18. Li, N., Wu, J. X., Ding, D., Cheng, J., Gao, N., and Chen, L. (2017) Structure of a pancreatic ATP-sensitive potassium channel. *Cell* **168,** 101.e10–110.e10
19. Martin, G. M., Yoshioka, C., Rex, E. A., Fay, J. F., Xie, Q., Whorton, M. R., Chen, J. Z., and Shyng, S. L. (2017) Cryo-EM structure of the ATP-sensitive potassium channel illuminates mechanisms of assembly and gating. *eLife* **6,** e24149
20. Männikkö, R., Jefferies, C., Flanagan, S. E., Hattersley, A., Ellard, S., and Ashcroft, F. M. (2010) Interaction between mutations in the slide helix of Kir6.2 associated with neonatal diabetes and neurological symptoms. *Hum. Mol. Genet.* **19,** 963–972
21. Masia, R., Enkvetchakul, D., and Nichols, C. G. (2005) Differential nucleotide regulation of K_{ATP} channels by SUR1 and SUR2A. *J. Mol. Cell. Cardiol.* **39,** 491–501
22. Proks, P., Antcliff, J. F., Lippiat, J., Gloyn, A. L., Hattersley, A. T., and Ashcroft, F. M. (2004) Molecular basis of Kir6.2 mutations associated with neonatal diabetes or neonatal diabetes plus neurological features. *Proc. Natl. Acad. Sci. U.S.A.* **101,** 17539–17544
23. Lin, Y. W., MacMullen, C., Ganguly, A., Stanley, C. A., and Shyng, S. L. (2006) A novel KCNJ11 mutation associated with congenital hyperinsulinism reduces the intrinsic open probability of β-cell ATP-sensitive potassium channels. *J. Biol. Chem.* **281,** 3006–3012
24. Enkvetchakul, D., Jeliazkova, I., Bhattacharyya, J., and Nichols, C. G. (2007) Control of inward rectifier K channel activity by lipid tethering of cytoplasmic domains. *J. Gen. Physiol.* **130,** 329–334
25. Rohács, T., Chen, J., Prestwich, G. D., and Logothetis, D. E. (1999) Distinct specificities of inwardly rectifying K^+ channels for phosphoinositides. *J. Biol. Chem.* **274,** 36065–36072
26. Enkvetchakul, D., and Nichols, C. G. (2003) Gating mechanism of K_{ATP} channels: function fits form. *J. Gen. Physiol.* **122,** 471–480
27. Reimann, F., Dabrowski, M., Jones, P., Gribble, F. M., and Ashcroft, F. M. (2003) Analysis of the differential modulation of sulphonylurea block of β-cell and cardiac ATP-sensitive K^+ (K_{ATP}) channels by Mg-nucleotides. *J. Physiol.* **547,** 159–168
28. Gribble, F. M., and Ashcroft, F. M. (1999) Differential sensitivity of β-cell and extrapancreatic K_{ATP} channels to gliclazide. *Diabetologia* **42,** 845–848
29. Loussouarn, G., Phillips, L. R., Masia, R., Rose, T., and Nichols, C. G. (2001) Flexibility of the Kir6.2 inward rectifier K+ channel pore. *Proc. Natl. Acad. Sci. U.S.A.* **98,** 4227–4232
30. Enkvetchakul, D., Loussouarn, G., Makhina, E., and Nichols, C. G. (2001) ATP interaction with the open state of the K_{ATP} channel. *Biophys. J.* **80,** 719–728
31. Lee, S. J., Ren, F., Zangerl-Plessl, E. M., Heyman, S., Stary-Weinzinger, A., Yuan, P., and Nichols, C. G. (2016) Structural basis of control of inward rectifier Kir2 channel gating by bulk anionic phospholipids. *J. Gen. Physiol.* **148,** 227–237
32. Guex, N., and Peitsch, M. C. (1997) SWISS-MODEL and the Swiss-Pdb-Viewer: an environment for comparative protein modeling. *Electrophoresis* **18,** 2714–2723
33. Wolf, M. G., Hoefling, M., Aponte-Santamaría, C., Grubmüller, H., and Groenhof, G. (2010) g_membed: efficient insertion of a membrane protein into an equilibrated lipid bilayer with minimal perturbation. *J. Comput. Chem.* **31,** 2169–2174
34. Berendsen, H. J., Grigera, J. R., and Straatsma, T. P. (1987) The missing term in effective pair potentials. *J. Phys. Chem.* **91,** 6269–6271
35. Lederer, W. J., and Nichols, C. G. (1989) Nucleotide modulation of the activity of rat heart ATP-sensitive K^+ channels in isolated membrane patches. *J. Physiol.* **419,** 193–211

ASBMB